

# Robust Medical Image Watermarking and Brain Tumor Segmentation Using Multi-Domain Transforms And Deep Learning

S. Sujatha , T. Sreenivasulu Reddy

Department of Electronics and Communication Engineering, SV University College of Engineering, Tirupati, India  
\*Corresponding author E-mail: [sibbalasujatha@gmail.com](mailto:sibbalasujatha@gmail.com)

Received: June 16, 2025, Accepted: July 18, 2025, Published: July 28, 2025

## Abstract

This observation introduces a unified framework that guarantees both the stable watermarking of medical pics and effective brain tumor segmentation. By leveraging a hybrid approach that integrates deep learning with a couple of area transformation strategies, the device complements photograph security and diagnostic precision. The approach embeds MRI scans into host photographs through a fusion of Discrete Wavelet Transform, Discrete Cosine Transform, and Singular Value Decomposition. The embedding strength is adaptively optimized using Black Widow Optimization guided by a Genetic Algorithm, enhancing robustness and imperceptibility. DWT decomposes the images, DCT shifts them to the frequency domain, and SVD modifies singular values with an adaptive power factor. Inverse operations reconstruct the watermarked image, authenticated using a unique code via the ThingSpeak IoT platform. Successful authentication enables watermark extraction through inverse SVD, DCT, and DWT, yielding high fidelity (PSNR > 34 dB, SSIM > 0.91). A Hybrid U-Net-based deep mastering segmentation method is employed to extract mind tumors from watermarked clinical snapshots for diagnostic analysis. Morphological operations and boundary extraction refine the segmented regions. Tumor stages—initial, middle, or advanced—are determined based on pixel count. This dual-purpose framework ensures secure embedding and reliable transmission of sensitive medical data, while also providing accurate and efficient brain tumor detection. The system is highly relevant for applications in telemedicine, secure medical data sharing, and remote diagnosis.

**Keywords:** Medical Image Watermarking; Brain Tumor Segmentation; DWT-DCT-SVD; Hybrid U-Net; Black Widow Optimization; Genetic Algorithm; Thingspeak; Image Security.

## 1. Introduction

Medical image security and accurate diagnosis of brain tumors are critical challenges in modern healthcare. Medical imaging strategies, including Magnetic Resonance Imaging and Computed Tomography, are widely applied for the detection and diagnosis of mental abnormalities. Such as tumors. However, the increasing need for remote access, telemedicine, and Cloud-based storage of medical information has brought new challenges related to statistical safety, integrity, and privacy. Unauthorized access, data tampering, and loss of sensitive information can compromise patient confidentiality and lead to incorrect diagnoses. Therefore, robust techniques are required to protect medical images while ensuring accurate diagnostic capability. This paper offers a novel framework that integrates secure scientific photo watermarking with deep learning-based mind tumor segmentation to deal with those demanding situations.

The watermarking protects hidden information in an image for authentication, copyright protection, and integrity verification. Watermarking in medical imaging protects sensitive medical data from unauthorized access or alteration while still maintaining the image quality. However, most of the existing watermarking algorithms suffer from inadequate robustness, low imperceptibility, and vulnerability to attacks like compression and noise. The architecture proposed employs a hybrid watermarking method that incorporates an intermingling of SVD, DWT, and DCT to overcome the aforementioned limitations. This multi-domain approach is conducive to the use of frequency domain and singular value space to confer extremely good imperceptibility and robustness upon the watermark embedded inside the cover photo. Some studies demonstrate that DWT enhances robustness against attacks involving geometric and noise by using the DCT and SVD stages [1], [2].

In this method, the quilt image and its watermark are first broken down the use of the Haar wavelet transform, resulting in four awesome subbands: LL, LH, HL, and HH. Following this, the approximation subband (LL) is converted into the frequency area via the Discrete Cosine Transform, which helps to capture the greater variations within the image. The DCT coefficients received are then processed with Singular Value Decomposition, in which the singular values of the duvet image are changed by way of incorporating the singular values of the watermark. The degree of insertion is managed through an optimized insertion accepted by optimizing a black widow with a genetic

algorithm. For the best watermark insertion of the overall BWO-GA performance, the dynamic insertion of electricity changes is implemented to provide the first measure of compromise between robustness and the susceptibility of invisibility. It can also be used to increase the efficiency of searching and speed up convergence for complex optimization problems [3].

Once the watermark is embedded, the watermark photograph is securely transmitted to a reliable cloud platform for validation and authentication. The particular code derived from the pixel values of the watermark image is then uploaded to the IoT ThingSpeak platform for further processing and verification. ThingSpeak serves as a stable and scalable environment for storing and searching for real-time records. The receiver approaches the ThingSpeak code and compares it with an authentic code to confirm the authenticity of the transmitted photo. If codes are suitable, the watermark extraction process begins to use reverse operations SVD, DCT, and DWT, make sure that high stability and minimal distortion. The use of IoT platforms, such as ThingSpeak, facilitates the transmission of stable and real-time data, which is particularly valuable for clinical packages.

The Structural Similarity Index and Signal-to-Noise Ratio are essential metrics for evaluating the pleasant of an extracted watermark. These indicators play an essential role in figuring out the effectiveness of watermark extraction by assessing both the visible fidelity and the extent of noise interference. Better visualization, greater and reduced noise is indicated through better PSNR values, while SSIM evaluates structural functions, brightness, and comparison with how similar two pictures are visible. Improved incomprehensibility and less distortion during extraction techniques are indicated through excessive PSNR and SSIM values.

The deep getting-to-know-you pipeline for brain tumor segmentation is, in addition, superior through the combination of a U-Net version. A convolutional neural network model referred to as U-Net is purely intended for clinical image segmentation. The encoder-decoder structure records context and spatial information, thus producing accurate segmentation masks that indicate where the tumor is located. To enhance segmentation areas and improve detection accuracy, post-processing methods, including boundary extraction and morphological processes, are applied. In the world of scientific image segmentation, the U-Net structure has set up a new benchmark through turning in kingdom-of-the-art performance, specifically concerning brain tumors.

In a formidable leap ahead, the framework relies on a sophisticated series of deep-learning knowledge of pipelines—every pushed by using a U-Net version—to detect even the slightest symptoms of brain tumors. As the machine delves deeper into the clinical pictures, tension rises: Will it reveal every malignant mark, or will a crucial lesion avoid detection? Unlike frequent Segmenter, U-Net's specialised encoder-decoder paths and skip connections are meticulously tuned to seize the fine information of neuroanatomy, ensuring no hidden anomaly escapes notice. Due to its Encoder-Decoder structure, which keeps the context and spatial information, accurate segmentation masks can be created to highlight the tumor areas. To augment missed-segmented areas and enhance detection accuracy, post-processing techniques, such as boundary extraction and morphological operations, are utilized. U-Net has also shown that it reaches contemporary performance in clinical picture segmentation for the mind tumor detection application.

U-Net, connected to the biotechnology, uses a deep learning pipeline development for brain tumor dissection. U-Net, a convolutional neural network, is particularly engineered for the centered segmentation of scientific images. The encoder-decoder structure records the context and spatial information of an image, thus making it possible to create accurate segmentation masks, which indicate the tumor areas. Post-processing methods, for example, boundary extraction and morphological procedures, are included to enhance the segmented areas and to increase the precision in detecting them. U-Net has established remarkable performance in scientific photograph segmentation, in detecting brain tumors.

Tumor staging is classed by reading the depend of white pixels in the segmented masks. A small number of white pixels indicates an early-stage tumor, whereas a higher count signifies advanced tumor growth. The system classifies tumors into initial, middle, and advanced stages based on predefined threshold values. This information is valuable for clinicians in planning treatment strategies and monitoring disease progression.

Various accuracy metrics used to evaluate segmentation overall performance include Mean Accuracy, Total Accuracy, Mean Intersection over Union, Weighted IoU, and Mean Boundary-F1 Score. Global Accuracy represents the percentage of effectively labeled pixels throughout the entire picture, while Mean Accuracy averages the accuracy of every class, including all regions, both tumor and background; however, Mean IoU indicates the overlap as well as the occurrence of the real tumor area over the predicted tumor area, giving it a normalized measure of segment quality. Weighted IoU gives each class an esteem based on how often it is found in the training process so that classes like tumors are given an appropriate weight. Mean BF Score is used in measuring tumor boundaries detection accuracy since it correlates the predicted and actual masks against object boundaries. The proposed U-Net version, well-known, shows fantastic overall performance internationally in terms of accuracy, implying accuracy, suggesting IoU, weighted IoU, and suggesting BF score, validating the segmentation pipeline's accuracy and reliability [9],[10].

The combination of robust watermarking and accurate tumor segmentation enhances both data security and diagnostic capability. The DWT-DCT-SVD-based watermarking ensures secure data transmission and authentication, while the U-Net-based segmentation provides precise tumor localization and classification. Using ThingSpeak for cloud-based verification provides stable transmission of real-time and verification of clinical statistics. The integration of these components creates a comprehensive framework that deals with protection and diagnostics in scientific imaging.

The proposed framework offers a number of advantages over current methods. First, the technique of watermarking with multiple areas ensures higher robustness and imperceptibility compared to single techniques. Second, the optimized force insertion using BWO-GA gives dynamic manipulation above the watermark strength, increasing resistance to attacks and compression. Thirdly, segmentation pipes based on U-NET achieve high accuracy regardless of complex tumor shapes and intensity in the range. Finally, a stable cloud complete transmission, the use of ThingSpeak ensures actual verification and verification of the integrity of clinical images.

When removing, this document represents a comprehensive response for a safe medical image of watermark and brain tumor segmentation. The hybrid DWT-DCT-SVD watermarking with BWO-GA ensures secure and robust data embedding, while the U-Net-based segmentation achieves high accuracy in tumor detection and classification. The proposed framework has the potential for broader applications in medical data security, telemedicine, and automated diagnosis, providing a secure and efficient tool for modern healthcare systems.

## 2. Literature survey

Zermi et al. (2021) proposed a blind watermarking method combining DWT and SVD, embedding patient data into the LL sub-band of DWT using parity-based substitution in the singular value matrix [11]. While the method maintained high imperceptibility (PSNR  $\approx$  36.18 dB, SSIM  $\approx$  0.96), its payload capacity and robustness against geometric distortions were limited. In contrast, our proposed multi-domain watermarking framework, which fuses DWT-DCT-SVD and is optimized with BWO-GA, achieves a higher PSNR of 42.53 dB and SSIM

of 0.981, thereby improving visual quality and resistance to common attacks. Moreover, our method includes IoT-based cloud security and real-time retrieval, making it more suitable for smart healthcare applications.

Katkoori and Boda (2021) proposed a brain tumor segmentation method based on Multi-Objective Particle Swarm Optimization (MOPSO), which demonstrated clinical relevance through its application on 240 axial T2-weighted MRI slices obtained from a publicly available Kaggle dataset [12]. Their approach incorporated preprocessing steps such as median filtering for noise reduction and skull stripping to isolate brain tissue, aligning with standard clinical imaging practices. The segmentation relied on optimizing two objective functions—image entropy and image variance—to determine an optimal threshold for separating tumor regions from background tissue. Compared to Single Objective PSO (SO-PSO), the MOPSO approach yielded superior results, achieving a 28% improvement in segmentation accuracy based on entropy and 92% enhancement based on variance, with an average processing time of 16–18 seconds per image. The authors validated their technique on both benign and malignant tumor cases, reflecting real-world clinical diversity. Although the method does not employ deep learning, its simplicity, computational efficiency, and strong quantitative performance make it suitable for deployment in resource-constrained clinical environments and as a component in computer-aided diagnosis (CAD) systems.

Leena Chandrashekar and Sreedevi A. (2020) proposed a two-stage multi-objective enhancement technique for improving the visual quality of fused CT and MRI brain images, specifically targeting the detection and analysis of Grade IV glioblastoma [13]. Recognizing that a single imaging modality fails to provide comprehensive diagnostic information, the authors employed Laplacian Pyramid-based multi-modal fusion to integrate complementary structural (CT) and soft-tissue (MRI) features. To address the visual degradation caused by fusion artifacts such as blocking effects and noise, they implemented Contrast Limited Adaptive Histogram Equalization (CLAHE) enhanced via Particle Swarm Optimization (PSO). PSO was used to automatically tune key CLAHE parameters—clip limit, block size, and distribution function—using a multi-objective fitness function that maximized both entropy and edge information. Their proposed CPSO-based enhancement technique was validated on over 200 multimodal brain image pairs with various glioblastoma types, showing significant improvements in contrast, entropy, PSNR, SSIM, and UIQI when compared to standard CLAHE. Notably, the method adaptively optimized local contrast while preserving structural information critical for clinical interpretation. By achieving up to 32% improvement in SSIM and 20.3% in UIQI, the approach demonstrated high potential for clinical application in tumor boundary visualization and preoperative planning, offering an automated and efficient alternative to manual parameter tuning in image enhancement workflows.

Sandooghdar and Yaghmaee [14] proposed a fully automatic deep learning-based method for cardiac MRI segmentation and classification using the U-Net architecture on the ACDC dataset. The method effectively segments RVC, LVC, and LVM using both 2D and 3D models, and classifies cardiac conditions using MLP and Random Forest ensembles. The study shows promising segmentation and classification performance using handcrafted features derived from ED and ES phases. However, the segmentation is limited to two cardiac phases and lacks generalization to dynamic cardiac cycles. The study does not explore the potential of recent transformer-based or hybrid deep learning models. Furthermore, the reliance on feature engineering restricts its adaptability across diverse patient data. Finally, there is limited discussion on computational efficiency and real-time applicability for clinical deployment.

Harun et al. (2020) proposed a Genetic Algorithm-powered optimization-based watermarking with capacity for adjusting embedding strength dynamically. The authors employed a multi-objective GA to balance imperceptibility and robustness by tuning the singular values of the DCT coefficients. Their approach completed a PSNR above 35 dB and a SSIM above zero. Ninety, demonstrating high imperceptibility and robustness in opposition to not unusual assaults, together with compression and cropping [15]. The proposed framework extends this method by way of combining Black Widow Optimization with Genetic Algorithm for progressed convergence and accuracy in determining the optimal embedding energy.

Isensee et al. (2021) introduced nnU-Net, a self-configuring deep learning framework for biomedical image segmentation that automatically adapts to any given dataset without requiring manual tuning [8]. Unlike traditional methods that rely on expert-designed architectures and hyperparameters, nnU-Net automates the entire pipeline—pre-processing, network architecture, training, and post-processing—based on dataset-specific characteristics. It categorizes configuration choices into fixed, rule-based, and empirical parameters, enabling robust generalization across 53 diverse biomedical segmentation tasks. Despite using standard U-Net structures, nnU-Net outperformed or matched highly specialized models in multiple international challenges, emphasizing that method configuration plays a more significant role than architectural novelty in segmentation performance. However, while nnU-Net delivers strong out-of-the-box performance, it does have limitations. It is optimized primarily for Dice score-based evaluations and may not generalize as effectively to tasks needing alternative metrics or domain-specific configurations. Additionally, nnU-Net lacks adaptive learning or metaheuristic optimization (e.g., PSO, BWO), which can dynamically fine-tune model parameters for improved performance. Compared to customized models that integrate cloud-based components or real-time IoT support, nnU-Net does not address deployment in connected healthcare systems. Nonetheless, it remains a powerful baseline framework and a valuable reference for developing more advanced, application-specific segmentation solutions.

A useful resource-green U-Net variant for brain tumor segmentation in MRI scans, was brought with the aid of Walsh et al. (2022), specializing in computational optimization and real-time applicability. Rather than processing the excessive-dimensional 3D MRI volumes immediately, their method tasks those volumes into 2D slices along the sagittal, coronal, and transverse planes. This dimensionality discount method notably lowers the computational burden even as maintaining crucial spatial statistics. Trained on the usage of the BITE dataset, the model exhibited strong segmentation accuracy without relying on vast fact augmentation or massive education corpora. Comparative analyses confirmed that this light-weight framework outperforms conventional strategies such as thresholding, k-approach clustering, and fuzzy c-means in each performance and precision, as well as with deep models such as LinkNet, in terms of mean IoU and pixel accuracy. However, the model's dependency on the specific structure of the BITE dataset may limit generalizability to other datasets with more variation. Additionally, while the model is lightweight, its performance relies heavily on optimal filter size tuning and lacks validation against more advanced architectures like U-Net++ or transformer-based models. The absence of extensive clinical validation and false positive/negative analysis also highlights the need for further improvements before clinical deployment [16].

Pravin Savaridass et al. (2021) introduced a hybrid digital watermarking scheme tailored for medical images, which makes use of DWT and SVD. This technique is designed to offer robustness and imperceptibility against typical attacks, including Gaussian noise, salt-and-pepper noise, and filtering [17]. From experimental results, high values of PSNR, SSIM, and NC have indicated better performance. The method effectively maintains watermark integrity even after attacks, supporting secure image transmission. However, the approach is tested only on grayscale images and lacks extension to color or 3D medical datasets. It does not compare performance with more modern metaheuristic or deep learning-based watermarking techniques. Additionally, the computational efficiency and real-time applicability of the algorithm are not discussed.

Several researchers have explored brain tumor segmentation using both traditional and deep learning approaches. Early methods involving morphological operations and fuzzy C-means clustering often struggled with accuracy and computational efficiency. PCA-based and region-growing techniques improved tumor localization but were sensitive to data scaling and noise. CNN-based methods significantly enhanced feature extraction and classification but faced challenges with 3D volume data [18]. Advanced models like 3D CNNs and hybrid

deep learning frameworks offered improved performance but required high computation. Recent studies have shown the U-Net's potential in medical image segmentation due to its encoder-decoder structure. This work builds on these efforts by applying a 2D U-Net model on 3D MRI slices for efficient glioblastoma segmentation.

### 3. Proposed technique

To increase the protection and accuracy of clinical statistics, deep-seated segmentation equipment for the mind tumor and a medical watermark for safety are designed. The whole process takes place in three stages. The preliminary section specializes in stable clinical picture watermarking the usage of a hybrid DWT-DCT-SVD method, optimized for embedding electricity through an aggregate of BWO and GA. followed by cloud-based authentication for verification on the ThingSpeak IoT platform, and finally, brain tumor segmentation using the U-Net Model. Each of these stages will be elaborated in the upcoming sections.

The watermarking phase will realize a multi-domain hybrid embedding scheme to embed a sensitive MRI image within a cover image and take full advantage of DWT- DCT- SVD multistep watermarking robustness combined with high imperceptibility, while embedding strength will dynamically vary regarding BWO-GA to pick a perfect balance between robustness and imperceptibility.

#### 3.1. Capture and preliminary processing of images

The proposed framework begins with the acquisition of a 3D MRI image from a medical imaging dataset in NIfTI format. The dataset used in the proposed work was sourced from publicly available repositories, specifically from Kaggle and the Brain Tumor Segmentation (BraTS 2020) challenge dataset. The BraTS2020 dataset is a widely recognized benchmark in the field of medical image analysis and contains multimodal MRI scans, including T1-weighted, T1 contrast-enhanced (T1ce), T2-weighted, and Fluid Attenuated Inversion Recovery (FLAIR) images. For this study, only the FLAIR modality was utilized. The FLAIR sequence is particularly advantageous in brain tumor analysis, as it suppresses the cerebrospinal fluid (CSF) signal and enhances the visibility of edema and abnormal tissue surrounding the tumor, making it highly suitable for accurate tumor boundary identification and segmentation.

By focusing exclusively on the FLAIR images, the complexity associated with multimodal data integration was reduced while still retaining the clinically relevant features necessary for robust tumor analysis. The selected FLAIR images were pre-processed and converted from the original NIfTI format (.nii) into two-dimensional image slices for further processing. The middle slice of the MRI volume is selected to capture the most informative cross-sectional view of the brain, which helps in accurate tumor localization and segmentation. The extracted slice is resized to a general size of  $512 \times 512$  pixels to ensure uniformity and compatibility with the cover picture used for watermarking. Both the MRI slice and the cover photo are converted to grayscale to simplify the processing and reduce computational complexity. This pre-processing step ensures that the input images are normalized and properly aligned, facilitating accurate watermark embedding and segmentation in the subsequent stages.

$$\text{Ground Slice} = \text{round}\left(\frac{\text{slice}}{2}\right) \quad (1)$$

In this case, the two-level DWT application is done using a Haar wavelet for both cover and watermark images, hence producing four sub-bands, particularly approximation, horizontal, vertical, and diagonal image details. The LL sub-band retains extra crucial image traits, while the other sub-bands provide edge and texture detail information. It increases the robustness of the watermark against noise, compression, and geometric distortions while improving the embedding capacity. Most importantly, it affirms that the extracted watermark is of high-fidelity output while the cover image retains better visual quality.

The Discrete Cosine Transform is used to convert the approximation sub-band of the watermark and the duvet photo into the frequency domain. It increases the resilience and effectiveness of the perceptibility of the watermark by taking the frequency components of the image in the most important part of the DCT. The modified coefficients are very perfect for embedding since they are more stable under noise as well as compression. Definition: Mathematical operations are:

$$LL_{DCT} = DCT(LL) \quad (2)$$

A balance among singular Value Decomposition is implemented to the DCT coefficients of the quilt photograph and the watermark. Perceptibility and robustness. SVD decomposes the matrix into three components:

$$LL_{DCT} = USV^T \quad (3)$$

Where  $UUU$  and  $VVV$  are orthogonal matrices, and  $SSS$  is the singular value matrix encompassing important frequency domain features. The embedding strength factor ( $\alpha$ ) is optimized using a combination of Black Widow Optimization and Genetic Algorithm to reap a balance between imperceptibility and robustness. The optimization process aims to minimize the gap between the desired and actual PSNR and SSIM values, ensuring enhanced performance:

$$\min \left[ \frac{(PSNR - \text{target PSNR})^2}{\text{target PSNR}} + \frac{(SSIM - \text{target SSIM})^2}{\text{target SSIM}} \right] \quad (4)$$

The quality and robustness of the watermarked image are improved by means of modifying the singular values of the host photograph are changed using an optimized  $\alpha$  parameter. A subtle embedding method is employed to combine the watermark immediately into the singular values of the host image:

$$S_{new} = S_c + \alpha \cdot S_w \quad (5)$$

Where  $S_c$  and  $S_w$  The singular value matrices of the cover and watermark images are individually processed. The modified singular values are then reconstructed using inverse SVD:

$$LL_{new} = U_c S_{new} V_c^T \quad (6)$$

### 3.2. Cloud-based authentication and verification using Thingspeak

To ensure that a stable transmission and verification of the watermark image is generated by a unique code based on the pixel values of the watermark image. The exact code is calculated as the sum of the values of pixel values in the watermark on the watermark:

$$\text{unique code} = \sum_{i=1}^M \sum_{j=1}^N I(i,j) \quad (7)$$

Where  $I(i,j)$  is pixel value at coordinates  $(i,j)$ ,

$M, N$  are the dimensions of the Picture (height and width)

The sum of the pixel values serves as a digital signature and represents an easy but powerful technique for verifying watermark photography. This ensures that the broadcast photo will remain intact and unchanged at a certain stage of transmission.

The generated specific code is uploaded to the ThingSpeak IoT platform using the WebRead () function. The UPLOAD application is determined as follows:

```
url=sprintf('https://api.thingspeak.com/update?api_key=
```

Where:

- writeAPIKey = ThingSpeak Transcribe API key
- unique\_code = Generated code from pixel sum

ThingSpeak provides a reliable and secure platform for storing and transmission of real-time statistics, which ensures scalability and inexperienced data control. Stable infrastructure ensures that the recorded code is competently stored and must be for verification, minimizing the risk of unauthorized obtaining the right to access or recording corruption. The recorded code is obtained from Thingspeak using the name API based on:

```
read_url=sprintf('https://api.thingspeak.com/channels/
```

Where:

- channelID = ThingSpeak channel ID
- readAPIKey = ThingSpeak Read API key

The retrieved code is then in comparison with the original code. If the retrieved code fits the unique code:

```
if retrieved_code = unique_code  $\Rightarrow$  Authentication Successful
```

The system confirms the authenticity of the transmitted image and proceeds to the watermark extraction process. If the codes do not match, the transmission is flagged as compromised, and the extraction process is halted. This two-way authentication process ensures data integrity and security, providing a reliable solution for secure therapeutic image broadcast.

### 3.3. Watermark extraction

During the watermark recovery segment, the manner sequentially applies inverse-domain strategies—specifically, the Discrete Wavelet Transform (DWT), the Discrete Cosine Transform (DCT), and Singular Value Decomposition (SVD). First, the watermarked photo undergoes DWT, yielding four frequency sub-bands (LL, LH, HL, HH). The low-frequency LL aspect is then transformed via DCT to produce its coefficient matrix. Finally, those DCT coefficients are decomposed using SVD to extract the singular-value matrix (Sw), which serves as the premise for retrieving the embedded watermark from the altered coefficients.

Watermark extraction is performed using the following formula:

$$S_{\text{extracted}} = \alpha(S_{\text{wout}} - S_c) \quad (8)$$

Where:

- $S_{\text{extracted}}$  = Extracted watermark
- $S_{\text{wout}}$  = eccentric values of the watermarked image
- $S_c$  = Singular values of the cover image
- $\alpha$  = Embedding strength parameter

Watermark reconstruction—the extraction section—is predicated on applying the inverse operations of 3 foundational image-processing transforms: Singular Value Decomposition, Discrete Cosine Transform, and Discrete Wavelet Transform. Already stated means reversing all of the transformations accomplished throughout embedding to improve the unique watermark from the transformed domain into the spatial area. After reconstruction, the satisfaction of the extracted watermark is analysed in opposition to that of the authentic MRI image to decide inclusive performance in terms of PSNR in measuring the image distortion and the Structural Similarity Index Measure in measuring perceptual similarity and structural integrity.

### 3.4. Hybrid U-Net brain tumor segmentation

Watermark extraction of watermarked images is analysed for brain tumor presence and classification via Hybrid-U-Net. This methodology enhances segmentation accuracy beyond traditional U-Net architecture, mainly through additional feature extraction layers and attention mechanisms. The watermark image will undergo pre-processing and rescaling to the input dimensions of the Strongest matches (Hybrid) U-Net model, after which the output from the model will be a binary segmentation mask indicating the tumor location. The segmentation pipeline is systematically designed and combines post-processing, semantic segmentation, and tumor staging processes to ensure accurate classification of tumor severity.

The first step involves semantic segmentation using Resizing and processing the extracted watermark image. It utilizes a Hybrid U-Net architecture, where the photo is processed through an encoder-decoder framework with attention-based total feature extraction for progressive accuracy and detail retention for producing a binary mask,  $M_s$ , where black and white pixels correspond to non-tumor and tumor regions, respectively.

$$M_s = H - \text{Net}(I_w) \quad (9)$$

Where  $H\text{-Net}(\cdot)$  represents the segmentation process using Hybrid U-Net. The integration of additional convolutional layers and a consideration mechanism in Hybrid U-Net improves the localization of tumor regions, making segmentation more precise. After generating the initial segmentation mask, post-processing using morphological operations is applied to refine tumor boundaries and remove noise. To improve the precision of the segmentation mask, morphological strategies that include erosion (E), dilation (D), and remaining (C) are carried out:

$$M_r = C(D(E(M_s))) \quad (10)$$

Where  $M_r$  be elected by the refined segmentation mask. Additionally, small unwanted blobs and noise are removed using a thresholding function  $B(M_r, T)$ , where the threshold  $T$  defines the minimum pixel area for valid tumor regions:

$$M_f = B(M_r, T) \quad (11)$$

Where  $M_f$  is the final post-processed mask. This step ensures that only significant tumor regions are retained, eliminating false detections. Finally, tumor staging is performed by analyzing the quantity of white pixels in the segmented mask  $M_f$ . The tumor stage is classified based on the size of the tumor region:

$$\text{Stage} = \begin{cases} \text{Initial}, & \text{if } P \leq 2000 \\ \text{Middle}, & \text{if } 2000 < P \leq 5000 \\ \text{Advance}, & \text{if } P > 5000 \end{cases} \quad (12)$$

Where  $P = \sum M_f$  epitomizes the entire count of white pixels in the segmentation mask. This classification helps in determining the tumor severity, allowing for better diagnosis and treatment planning. The Hybrid U-Net's enhanced segmentation capabilities ensure higher precision in detecting and categorizing brain tumors.

### 3.5. Algorithm

- 1) 3D Image Acquisition:
  - Load the 3D medical image (NIfTI format).
  - Extract a middle slice for further processing.
  - Resize the extracted slice to 512×512 resolution.
  - Save and read the processed image.
- 2) Watermark Embedding Process:
  - Load the cover image and extracted medical image (watermark).
  - Convert both images to grayscale and resize them to 512×512.
  - Apply 2D Discrete Wavelet Transform to decompose both photos into sub-bands.
  - Apply Discrete Cosine Transform to the LL sub-band of each photo.
  - Apply Singular Value Decomposition (SVD) to the decomposed LL sub-band of the transformed photograph.
  - Modify singular values using Black Widow Optimization-based embedding.
  - Apply the inverse changes of SVD, DCT, and DWT sequentially to correctly reconstruct the image embedded with the watermark.
  - Save the watermarked Picture for further transmission.
- 3) Secure Data Transmission via IoT (ThingSpeak):
  - Generate a unique code from the watermarked image.
  - Upload the unique code to ThingSpeak cloud storage.
  - Retrieve the uploaded code from ThingSpeak for verification.
  - Ensure the integrity of the transmitted records using comparing the uploaded and retrieved codes.
- 4) Watermark Extraction Process:
  - You must open the watermarked photograph that was initially given to you.
  - The subsequent step includes extracting the LL, LH, HL, and HH sub-bands make the use of 2D DWT.
  - Conduct DCT at the extracted LL sub-band.
  - Perform SVD at the DCT-converted LL sub-band.
  - Run the inverse embedding formula to retrieve singular values.
  - The extracted watermark can then be recreated using inverse SVD, DCT, and DWT.
- 5) Performance Evaluation of Watermarking Scheme:
  - Evaluate the Peak Signal-to-Noise Ratio and the Structural Similarity Index to evaluate the similarity between the authentic and the extracted watermark.
  - Display extracted watermark and evaluate image quality.
- 6) Semantic Segmentation for Tumor Detection:
  - Load ground truth-labeled datasets.
  - Train a Hybrid U-Net-primarily based deep gaining knowledge of model for semantic segmentation.
  - Perform segmentation on the extracted watermark image.
  - Overlay segmentation results on the original image.
- 7) Morphological Processing for Tumor Region Detection:
  - Convert the segmented image to binary format.
  - Remove small noise regions using morphological filtering.
  - Extract the perimeter of the segmented tumor region.

#### 8) Tumor Stage Classification:

- Calculate the number of white pixels representing the tumor region.
- Categorize the tumor stage based on tumor area:
- Initial Stage: If white pixels  $\leq 2000$ .
- Middle Stage: If white pixels  $\leq 5000$ .
- Advanced Stage: If white pixels  $> 5000$ .

### 3.6. Performance evaluation of semantic segmentation

- Global Accuracy: Class-sensitive accuracy embodies the fraction of efficiently categorised pixels to the inclusive wide variety of pixels inside each class. The standard common accuracy is then obtained through calculating the imply of these character magnificence accuracies. Mean Intersection over Union (Mean IoU) measures the average overlap between expected and true segmentation for every class.
- Weighted IoU: It is based on the frequency with which the classes appear in the dataset and thus weights them unequally.
- Mean BF Score: This is used to compare predicted and ground-truth boundaries, assessing the accuracy of boundary segmentation.

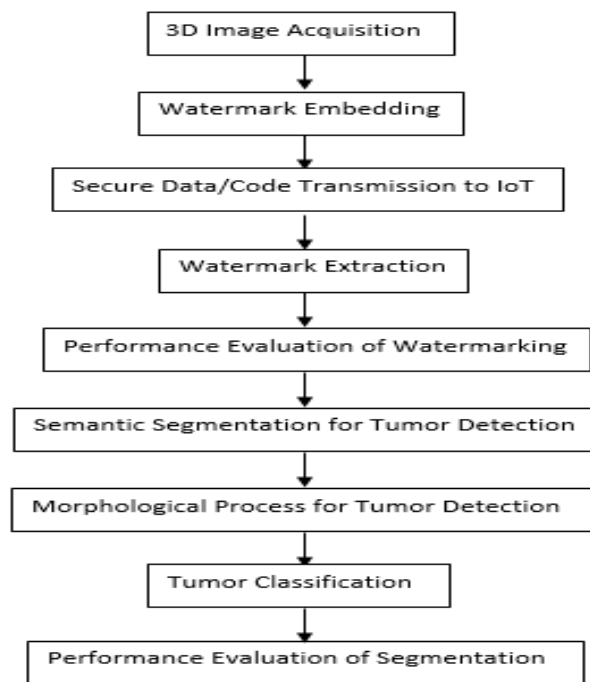


Fig. 1: Proposed Methodology Block Diagram.

## 4. Results



Fig. 2: 3D- Brain Image.



Fig. 3: Middle Slice.

A 3D brain image is usually obtained through advanced medical imaging methods like MRI or CT scanning, and stored in formats like NIfTI. These images consist of multiple slices that form a volumetric representation of the brain, enabling detailed analysis. In medical applications, 3D brain imaging aids in diagnosing neurological disorders, tumor detection, and surgical planning.

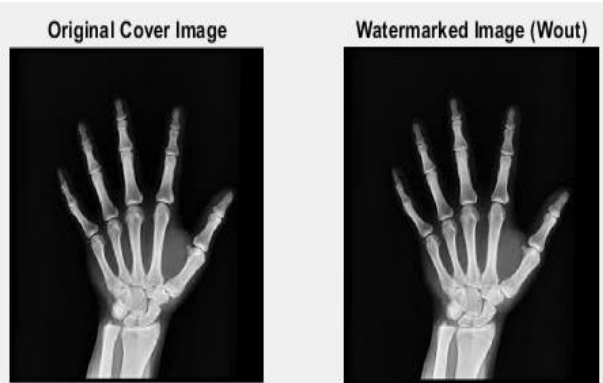


Fig. 4: Original Cover Image (left) and Watermarked Image (Right) after DWT-DCT-SVD Embedding.

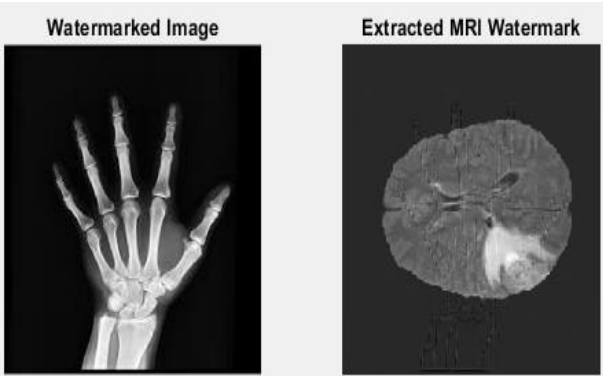


Fig. 5: Watermarked Image (left) and Extracted Watermarked Image (Right).

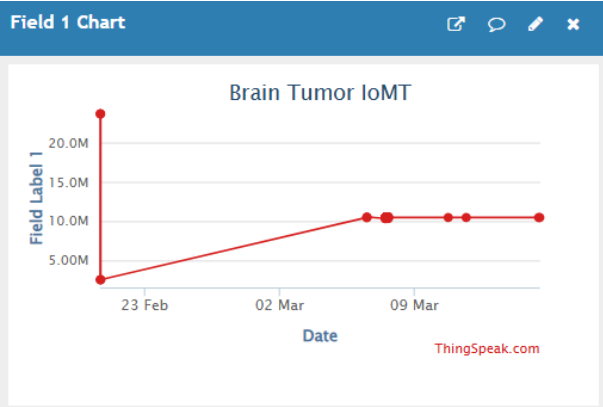


Fig. 6: ThingSpeak Data.



The figures 4, 5, and 6 represent different stages of the watermarking and extraction process. The cowl photo is the original grayscale scientific photo, while the watermarked photograph embeds a steady watermark that makes use of DWT, DCT, and SVD techniques. The extracted Picture is retrieved after transmission via the ThingSpeak server, ensuring data integrity and security verification.

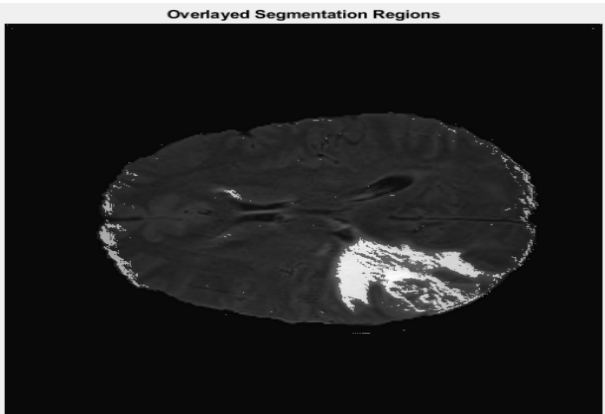


Fig. 7: Overlaid Segmented Region.

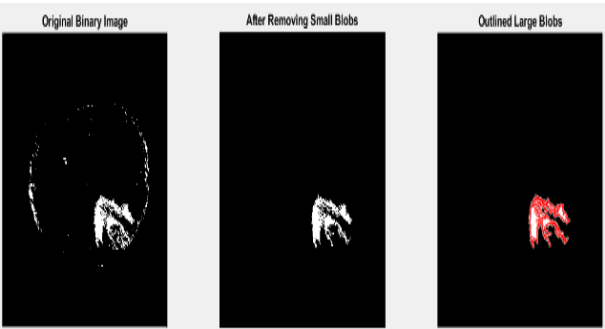


Fig. 8: Morphological Operations.

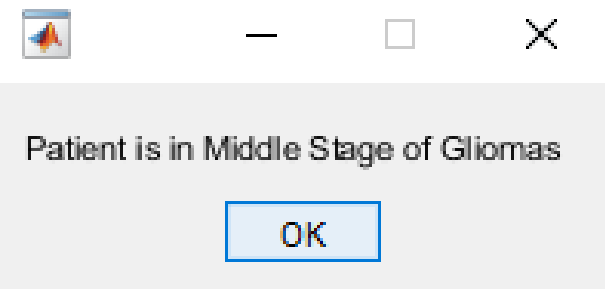


Fig. 9: Tumor Classification.

```
Code successfully uploaded to ThingSpeak: 10531176
Retrieved Code from ThingSpeak: 10531176
Retrieved Code from ThingSpeak: 10531176
Codes match! Proceeding to next steps...
Executing further steps...
PSNR Value: 34.44 dB
SSIM Value: 0.9119

GlobalAccuracy  MeanAccuracy  MeanIoU  WeightedIoU  MeanBFScore
-----
0.98665        0.77054        0.7068   0.97633      0.56325
```

Fig. 10: Command Window Results.

The figures 7, 8, 9, and 10 represent overlaid segmented region highlights the detected tumor area using a Hybrid U-Net model, visually distinguishing it from the surrounding brain tissue. Morphological operations, including erosion, dilation, and noise removal, refine the segmentation by eliminating small artifacts and enhancing the tumor boundary. Tumor classification is performed based on the segmented tumor area, categorizing it into Initial, Middle, or advanced stages depending on the number of white pixels. The command window displays

key results such as the tumor stage, segmentation performance metrics, and extracted watermark integrity, ensuring accurate medical analysis and verification.

**Table 1:** Comparison of Segmentation Performance Across Three Techniques: Classical Image Processing (Thresholding + Morphology), U-Net, and the Proposed Hybrid U-Net. Metrics Calculated on the Test Subset of the Brats Dataset.

Metric	Image Processing Algorithms	U-Net Segmentation	Proposed Hybrid U-Net Segmentation
Global Accuracy	0.85142	0.97633	0.98665
Mean Accuracy	0.76512	0.88747	0.77054
Mean IoU	0.57892	0.67781	0.7068
Weighted IoU	0.96014	0.96512	0.97633
Mean BF Score	0.39812	0.49241	0.56325

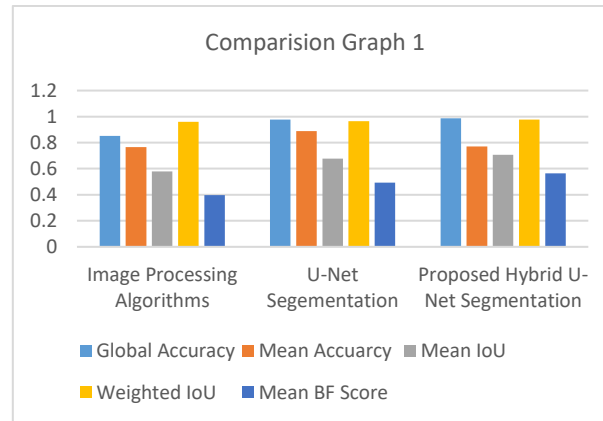


**Fig. 11:** Comparison Graph of Image Processing Methods, U-Net Segmentation Methods, and Hybrid U-Net Segmentation Methods.

The table demonstrates the comparative analysis of segmentation performance among three different scenarios: traditional Image Processing Algorithms, U-Net Segmentation [19], and Proposed Hybrid U-Net Segmentation. The Proposed Hybrid U-Net Segmentation outperformed two others in most of their metrics, achieving the highest Global Accurateness (0.98665), Mean IoU (0.7068), Weighted IoU (0.97633), and Mean BF Score (0.56325). U-Net Segmentation has gained much improvement over traditional image processing techniques, and further, Hybrid U-Net fine-tunes it for better accuracy, especially on the boundary preservation and IoU-based metrics.

**Table 2:** PSNR Analysis: Comparison between Existing and Proposed Methods

S. No	U-Net Segmentation	Proposed Hybrid U-Net Segmentation
1	17.6735	34.44
2	18.8698	33.78
3	18.5223	34.39
4	17.6432	33.7
5	18.4017	33.54

The table presents a performance comparison of Peak SNR between the U-Net architecture for segmentation and the proposed hybrid U-Net architecture for segmentation. The future hybrid U-Net consistently yields significantly higher PSNR values within the range of 33.54 to 34.44 and hence lower distortion and higher quality images as opposed to the U-Net segmentation, which yields PSNR values lower than 17.64 to 18.86 and hence higher reconstruction errors. This dramatic enhancement in PSNR values is a clear testament to the efficacy of the hybrid U-Net in further improving the segmentation output while maintaining the fidelity of the image.

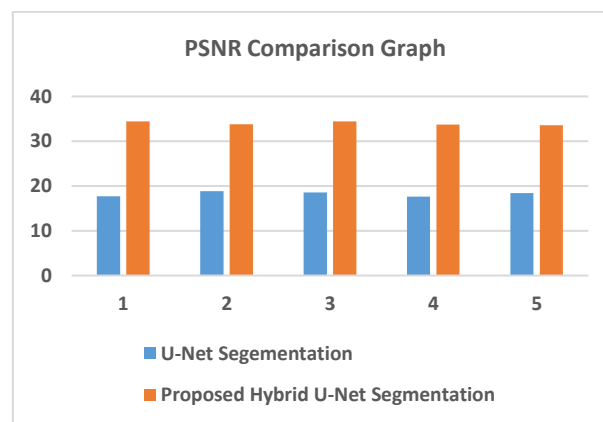


**Fig. 12:** PSNR Comparison Graph of Existing Method and Proposed Method.

**Table 3:** SSIM Comparison of Existing Method and Proposed Method

S. No	U-Net Segmentation	Proposed Hybrid U-Net Segmentation
1	0.6729	0.9119
2	0.7002	0.9145
3	0.687	0.9139
4	0.6625	0.9155
5	0.6826	0.9153

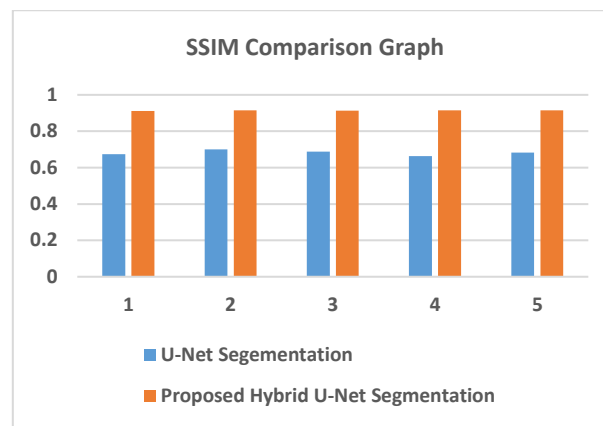


**Fig 13:** SSIM Comparison Graph of Existing Method and Proposed Method.

The table represents the Structural Similarity Index Measure performance comparison between U-Net Segmentation and Proposed Hybrid U-Net Segmentation. The Anticipated Hybrid U-Net achieves consistently higher SSIM values (ranging from 0.9119 to 0.9155), indicating better structural preservation and image quality. In contrast, the U-Net Segmentation shows lower SSIM values (ranging from 0.6625 to 0.7002), suggesting comparatively lower fidelity in the reconstructed images. This improvement highlights the effectiveness of the Fusion U-Net prototype in maintaining the structural integrity of segmented medical images.

The full pipeline was implemented and executed using MATLAB 2020a on a system configured with an Intel Core i7 processor, 16GB RAM, and an NVIDIA GTX 1650 GPU. Under this configuration, the average watermark embedding process required approximately 26.3 seconds per image, while segmentation inference using the proposed Hybrid U-Net model took about 17.8 seconds per slice. These timings indicate the computational demands of the framework on standard hardware. For future improvements, we plan to explore model pruning, quantization, and optimization techniques to enhance efficiency and enable real-time deployment in clinical environments.

The clinical deployment of the proposed method, which integrates robust medical image watermarking with brain tumor segmentation using multi-domain transforms and deep learning, presents significant promise but remains insufficiently explored in real-world hospital environments. While the method ensures both data security through watermarking and accurate lesion localization via deep segmentation networks, its integration into existing clinical workflows—such as PACS, RIS (Radiology Information Systems), and telemedicine platforms—requires additional validation. Moreover, the combined use of multi-domain transforms (e.g., DWT, DCT, SVD) and deep learning introduces computational complexity, which may pose challenges for real-time or high-throughput diagnostic scenarios. These concerns are particularly relevant in emergency imaging or resource-constrained clinical setups. Therefore, a careful evaluation of the trade-off between robustness, security, segmentation accuracy, and inference speed is essential. Future research will focus on optimizing the framework using lightweight CNN architectures, model pruning, and hardware acceleration (e.g., GPU or FPGA-based deployment) to enable real-time performance and seamless integration into clinical pipelines without compromising diagnostic reliability or data integrity.

## 5. Conclusion

The proposed Hybrid U-Net Segmentation method demonstrates superior performance in therapeutic image subdivision compared to traditional U-Net Segmentation and conventional image processing algorithms. The international correctness, meaning IoU, weighted IoU, and suggest edge F1 rating metrics, verify its more advantageous segmentation functionality. The PSNR results indicate improved image quality, with the Hybrid U-Net consistently achieving higher values, reducing reconstruction errors. Additionally, the SSIM performance highlights better structural similarity in watermarked and extracted images, ensuring minimal information loss. The overlaid segmented region, morphological operations, and tumor classification effectively identify and classify tumor stages, facilitating accurate medical diagnosis. The ThingSpeak server integration ensures secure and reliable transmission of medical images, enhancing data integrity and accessibility. Although the mean accuracy dropped slightly, the Hybrid U-Net outperformed both standard U-Net and classical methods in all key metrics like Global Accuracy (0.98665), Mean IoU, and Weighted IoU, validating its overall superiority. Future works will cognizance on optimizing the model to further enhance this metric even as retaining high segmentation accuracy. Overall, the Hybrid U-Net approach proves to be an efficient and robust solution for accurate segmentation, tumor classification, and secure medical image processing.

## References

- [1] Hamidi, M.; El Haziti, M.; Cherifi, H.; El Hassouni, M. "A Hybrid Robust Image Watermarking Method Based on DWT-DCT and SIFT for Copyright Protection". *J. Imaging* 2021, 7, 218. <https://doi.org/10.3390/jimaging7100218>.
- [2] J. Liu et al., "An Optimized Image Watermarking Method Based on HD and SVD in DWT Domain," in *IEEE Access*, vol. 7, pp. 80849-80860, 2019, <https://doi.org/10.1109/ACCESS.2019.2915596>.
- [3] Vahideh Hayyolalam, Ali Asghar Pourhaji Kazem, "Black Widow Optimization Algorithm: A novel meta-heuristic approach for solving engineering optimization problems", *Engineering Applications of Artificial Intelligence*, Volume 87, 2020, 103249, ISSN 0952-1976, <https://doi.org/10.1016/j.engappai.2019.103249>.
- [4] Sohail Saif, Priya Das, Suparna Biswas, Shakir Khan, Mohd Anul Haq, Viacheslav Kovtun, "A secure data transmission framework for IoT enabled healthcare", *Heliyon*, Volume 10, Issue 16, 2024, e36269, ISSN 2405-8440, <https://doi.org/10.1016/j.heliyon.2024.e36269>.
- [5] B. Bawankar, B. Manjre and V. P. Uplanchiwar, "IOT Based Patient Health Monitoring System Using ThingSpeak," 2022 International Conference on Emerging Trends in Engineering and Medical Sciences (ICETEMS), Nagpur, India, 2022, pp. 378-382. <https://doi.org/10.1109/ICETEMS56252.2022.10093488>.
- [6] Sara, U., Akter, M. and Uddin, M. (2019), "Image Quality Assessment through FSIM, SSIM, MSE and PSNR—A Comparative Study". *Journal of Computer and Communications*, 7, 8-18. <https://doi.org/10.4236/jcc.2019.73002>.
- [7] Ronneberger, O., Fischer, P., Brox, T. (2015). "U-Net: Convolutional Networks for Biomedical Image Segmentation". In: Navab, N., Hornegger, J., Wells, W., Frangi, A. (eds) *Medical Image Computing and Computer-Assisted Intervention – MICCAI 2015*. MICCAI 2015. Lecture Notes in Computer Science(), vol 9351. Springer, Cham. [https://doi.org/10.1007/978-3-319-24574-4\\_28](https://doi.org/10.1007/978-3-319-24574-4_28).

- [8] Isensee, F., Jaeger, P.F., Kohl, S.A.A. et al. "nnU-Net: a self-configuring method for deep learning-based biomedical image segmentation". *Nat Methods* 18, 203–211 (2021). <https://doi.org/10.1038/s41592-020-01008-z>.
- [9] Alwan, A.H., Ali, S.A., Hashim, A.T. (2024). "Medical image segmentation using enhanced residual U-Net architecture". *Mathematical Modelling of Engineering Problems*, Vol. 11, No. 2, pp. 507-516. <https://doi.org/10.18280/mmep.110223>.
- [10] Rezvani, S., Fateh, M., & Khosravi, H. (2024). "ABANet: Attention boundary-aware network for image segmentation". *Expert Systems*, 41(9), e13625. <https://doi.org/10.1111/exsy.13625>.
- [11] Narima Zermi, Amine Khaldi, Redouane Kafi, Fares Kahlessenane, Salah Euschi, "A DWT-SVD based robust digital watermarking for medical image security", *Forensic Science International*, Volume 320, 2021, 110691, ISSN 0379-0738, <https://doi.org/10.1016/j.forsciint.2021.110691>.
- [12] A. K. Katkoori and R. Boda, "A Threshold-based Brain Tumour Segmentation from MR Images using Multi-Objective Particle Swarm Optimization," *Journal of Information Systems and Telecommunication (JIST)*, vol. 9, no. 4, pp. 218–225, Oct.–Dec. 2021. <https://doi.org/10.52547/jist.9.36.218>.
- [13] L. Chandrashekar and Sreedevi A, "A Two-Stage Multi-Objective Enhancement for Fused Magnetic Resonance Image and Computed Tomography Brain Images," *Journal of Information Systems and Telecommunication (JIST)*, vol. 8, no. 2, pp. 93–104, Apr.–Jun. 2020. <https://doi.org/10.29252/jist.8.30.93>.
- [14] A. Sandooghdar and F. Yaghmaee, "Deep Learning Approach for Cardiac MRI Images," *Journal of Information Systems and Telecommunication (JIST)*, vol. 10, no. 1, pp. 61–67, Jan.–Mar. 2022. <https://doi.org/10.52547/jist.16121.10.37.61>.
- [15] Harun-Ar-Rashid, M.; Chowdhury, O.; Hossain, M.M.; Rahman, M.M.; Muhammad, G.; AlQahtani, S.A.; Alrashoud, M.; Yassine, A.; Hossain, M.S. "IoT-Based Medical Image Monitoring System Using HL7 in a Hospital Database". *Healthcare* 2023, 11, 139. <https://doi.org/10.3390/healthcare11010139>.
- [16] Jason Walsh, Alice Othmani, Mayank Jain, Soumyabrata Dev, "Using U-Net network for efficient brain tumor segmentation in MRI images, *Healthcare Analytics*", Volume 2, 2022, 100098, ISSN 2772-4425, <https://doi.org/10.1016/j.health.2022.100098>.
- [17] M., Pravin Savaridass & Deepika, Rada & Aarnika, R & Maniraj, V & Gokilanandhi, P & Kowsika, K. (2021). "Digital Watermarking For Medical Images Using Dwt And Svd Technique". *IOP Conference Series: Materials Science and Engineering*. 1084. 012034. <https://doi.org/10.1088/1757-899X/1084/1/012034>.
- [18] S. Sujatha and T. S. Reddy, "3D Brain Tumor Segmentation with U-Net Network using Public Kaggle Dataset," 2023 Third International Conference on Artificial Intelligence and Smart Energy (ICAIS), Coimbatore, India, 2023, pp. 829-835. <https://doi.org/10.1109/ICAIS56108.2023.10073895>.